

Characteristics of ordinary mode in fully relativistic electron plasma

Waseem Khan¹ , M Ali²  and Yousaf Habib³ 

¹ Department of Physical Electronics Faculty of Science, Masaryk University, Kotlářská 2, 61137 Brno, Czech Republic

² School of Natural Sciences (SNS), National University of Sciences and Technology (NUST), 44000 Islamabad, Pakistan

³ Department of Mathematics, COMSATS University Islamabad, Lahore Campus, 54000 Lahore, Pakistan

Received 1 December 2019, revised 15 March 2020

Accepted for publication 19 March 2020

Published 20 April 2020



Abstract

Propagation characteristics (resonances, propagation regions, and cutoffs) of ordinary waves (perpendicularly propagating electromagnetic waves) are studied in a relativistic electron plasma by using the kinetic model. The dispersion relation for the ordinary mode (O-mode) in a relativistic electron plasma is investigated by employing the Maxwell-Boltzmann-Jüttner distribution function. As the integration in the relativistic dispersion relation cannot be done analytically so an approximated value is obtained using the trapezoidal rule. Various modes of propagation for the ordinary waves are observed for each harmonic number n due to the relativistic effects defined by the value $\eta = \frac{mc^2}{k_B T_e}$. We also observe that the high-temperature relativistic plasma environment is more transparent for the O-mode as compared to weakly relativistic and non-relativistic plasma environments. Moreover, the cutoff points are shifted to lower values in the relativistic limit.

Keywords: resonances, propagation regions, cutoffs, ordinary waves, relativistic plasma, tokamak, cyclotron harmonic

(Some figures may appear in colour only in the online journal)

1. Introduction

Various plasma environments that exist in different regions of the Universe can be classified as being non-relativistic, weakly relativistic, relativistic, degenerate, relativistic degenerate, magnetized, cold and hot depending on the plasma parameters like density, magnetic field, and temperature. These parameters vary over a wide range, so the characteristics of the dispersion curves of a wave get modified by changing the plasma environment. The relativistic plasmas exist in many astrophysical objects (pulsars, quasars, active galactic nuclei, black holes, white dwarfs, neutron stars and radio galaxies) and laboratory environments (fusion experiment). The environments where a plasma contains particles with high thermal velocities, the relativistic effects play an important role in the dispersion curves of the waves. The characteristics (excitation, propagation, absorption, cutoff, harmonic structure) of electromagnetic waves in magnetized plasmas require precise measurement of the relativistic effects associated

with the fast-moving electrons, especially for perpendicularly propagating modes (O-mode, X-mode and Bernstein waves) as they all lie in the electron cyclotron resonance frequency range. These waves are used for electron cyclotron resonance heating and current drive in the tokamaks [1–15]. The electromagnetic waves for which the perturbed electric field \mathbf{E}_1 is parallel to the ambient magnetic field \mathbf{B}_0 ($\mathbf{E}_1 \parallel \mathbf{B}_0$) and the propagation vector k is perpendicular to the ambient magnetic field ($\mathbf{k} \perp \mathbf{B}_0$) are called the ordinary waves. These waves can be studied either by the fluid theory or the kinetic theory. According to the fluid theory, these waves remain unaffected by the magnetic field since we average over Larmor orbit. In order to observe the magnetic field effects on these waves, we use the kinetic model and these effects become significant when we include higher harmonics of the cyclotron frequency. The ordinary mode (O-mode) is an important wave for cyclotron heating of the magnetically confined plasma and for ionospheric heating experiments [16–22]. These waves are strongly absorbed in hot plasma, so they are emitted as

blackbody radiations and can be used to measure the local electron temperature in a tokamak plasma [23]. Many authors have studied different characteristics (growth rate, damping, and propagation) of the O-mode in different plasma environments. S. Zaheer and G. Murtaza studied the growth rate and propagation characteristics of the O-mode in a homogeneous relativistic plasma environment. They observe that the non-propagation region disappears as we increase the values of the harmonic number n as well as the damping rate depends directly on n [24]. R A Lopez *et al* analyze the dispersion relation for the O-mode in an electron-positron pair plasma and they observe that the effective plasma frequency (the lower cutoff for the electromagnetic branch) decreases with the increase in temperature [25]. Z Iqbal *et al* studied this wave in degenerate anisotropic plasma. It was observed that a new banded type of instability gets excited, which needs some particular values of temperature anisotropy and external magnetic field to grow [26]. K Azra *et al* studied the propagation characteristics of the O-mode in a relativistic degenerate electron plasma and examined the behavior of the wave by taking different values of the plasma density and magnetic field that corresponds to a particular astrophysical environment. They concluded that the cutoff and the resonance points are shifted to lower values of frequency due to relativistic effects [27]. G Abbas *et al* derived the dispersion relations for the perpendicular propagating modes (X-mode, O-mode and upper hybrid mode) for a weakly magnetized relativistic degenerate electron plasma and they found that due to the relativistic effects, the characteristics of the dispersion, cutoff and resonance points are shifted to the lower values of frequency resulting in enhancement of the propagation domain [28].

In the above mentioned literature, we have presented the findings of some of the authors about the propagation of the ordinary waves in various plasma environments. Many others [40–42] have put in a great effort to understand the behavior of these waves in the relativistic magnetized plasma. M Ali *et al* studied the propagation of O-mode in ultra-relativistic Maxwellian electron plasma and they found that the damping rate does not increase indefinitely for small wave number instead the damping is constrained in the presence of strong magnetic field [29]. L Nikolic and S Pesic [30] have discussed ordinary waves in a relativistic plasma by using I. Weiss approach [43]. In this approach, all infinite harmonics represented in a single term and denominator passes via zero for every ω^* that is an integer. They examined the variation in the real and imaginary part of the refractive index with the normalized frequency ($\frac{\omega_{ce}}{\omega}$) for non-relativistic, weakly relativistic and relativistic temperatures, along with several values of density. It was observed that as the electron temperature increases the cyclotron harmonic resonances get broaden due to relativistic effects. The real part of the refractive index increases with increasing the electron temperature and gradually it reaches its free-space value. They also observed a shift in the maximum value of the imaginary part of refractive index with an increase in the density.

To complete the analysis we will choose the value of $\eta = \frac{mc^2}{k_B T_e}$ (ratio of the rest mass energy to the thermal) that will decide whether we are in a relativistic ($\eta \leq 1$), weakly relativistic ($\eta > 1$) or non-relativistic ($\eta \gg 1$) environment [2, 21]. As we are trying to understand the dependence of the harmonic structure of O-mode on the relativistic momentum and propagation of the wave at each harmonic of the cyclotron frequency, we use the generalized expression for the O-mode derived by A Kalsoom *et al* [27] leads to an infinite sum of terms, each of which has a Bessel function which contains momentum as its argument and that is integrated over the momentum space. The plan of this paper is as follows: In section 2, the general dispersion relation for the ordinary waves in relativistic electron plasma is given. In section 3, a numerical approach is presented for the approximate solution of the integrand in the dispersion relation for O-mode. In section 4, discussion and graphical analysis are given and finally in section 4.1, the conclusion of our work is presented.

2. The generalized expression for the ordinary waves.

The generalized expression for the ordinary waves in a relativistic electron plasma is given as [27],

$$\begin{aligned} \omega^2 = c^2 k_x^2 + \left(\frac{16\pi^2 e^2 n_0}{3\omega} \right) \int_0^\infty v p^2 \frac{\partial f_o}{\partial p} {}_1F_2 \left[\left(\frac{1}{2} \right); \left(\frac{5}{2}, 1 \right); \right. \\ \left. - \left(\frac{k_x v}{\Omega} \right)^2 \right] dp + \sum_{n=1}^\infty \frac{16\pi^2 e^2 n_0}{(2n+3)\Gamma(2n+2)} \int_0^\infty v p^2 \frac{\partial f_o}{\partial p} \left(\frac{k_x v}{\Omega} \right)^{2n} \\ \times \left(\frac{1}{w-n\Omega} + \frac{1}{w+n\Omega} \right) {}_1F_2 \left[\left(\frac{1}{2} + n \right); \left(\frac{5}{2} + n, 1 + 2n \right); \right. \\ \left. - \left(\frac{k_x v}{\Omega} \right)^2 \right] dp. \end{aligned} \quad (1)$$

Here e , n_0 , Ω , f_o , n and ${}_pF_q[(a_1, \dots, a_p), (b_1, \dots, b_q), x]$ are the electron charge, equilibrium number density, relativistic cyclotron frequency, equilibrium distribution function, the harmonic number and a generalized Hyper-geometric function respectively [2, 21, 27, 32].

To account for the relativistic effects on the dispersion curves [2, 21, 33, 34, 44] we use the Maxwell-Jüttner equilibrium distribution function which is given as,

$$f_0(\mathbf{p}) = \frac{1}{4\pi m^3 c^3} \frac{\eta}{K_2(\eta)} \exp[-\eta\gamma], \quad (2)$$

where the relativistic factor γ is defined as,

$$\gamma = \left(1 + \frac{p^2}{m^2 c^2} \right)^{\frac{1}{2}},$$

and K_2 is the modified Bessel function of the second kind of order two. By substituting the relativistic distribution function in equation (1), we get,

$$\omega^2 = c^2 k_x^2 + \omega_{pe}^2 \frac{\eta^2}{K_2(\eta)} \times I_1 + 2\omega^2 \omega_{pe}^2 \frac{\eta^2}{K_2(\eta)} \times \sum_{n=1}^{\infty} \frac{\left(\frac{ck_x}{\omega_{ce}}\right)^{2n}}{(2n+3)\Gamma(2n+2)} \times I_2, \quad (3)$$

$$I_1 = \int_0^{100} \frac{z^4 \exp[-\eta(1+z^2)^{\frac{1}{2}}]}{1+z^2} \times {}_1F_2\left[\left(\frac{1}{2}\right); \left(\frac{5}{2}, 1\right); -z^2 \left(\frac{ck_x}{\omega_{ce}}\right)^2\right] dz \quad (4)$$

$$I_2 = \int_0^{100} \frac{z^{2n+4} \exp[-\eta(1+z^2)^{\frac{1}{2}}]}{\left((1+z^2)\omega^2 - n^2\omega_{ce}^2\right)} \times {}_1F_2\left[\left(\frac{1}{2} + n\right); \left(\frac{5}{2} + n, 1 + 2n\right); -z^2 \left(\frac{ck_x}{\omega_{ce}}\right)^2\right] dz \quad (5)$$

$$z = \frac{p}{mc}.$$

3. Numerical Approach

The integrals given by equations (4) and (5) have no explicit anti-derivatives. The numerical quadrature is one of the promising methods for definite integrals of a function having no explicit anti-derivative or not easy to obtain in terms of elementary functions. The idea is to evaluate the integrand function on a finite set of points within the interval of integration and then obtain a weighted sum of these function values to obtain an approximation of the definite integral. The integration points and the weights depend on the specific method used. Here we have employed trapezoidal method whose general formula is,

$$\int_a^b f(x) dx \approx \sum_{n=1}^M \frac{f(x_{n-1}) - f(x_n)}{2} \Delta x_n.$$

The interval of integration $[a, b]$ is partitioned into finite set of points $a = x_0 < x_1 < \dots < x_M = b$ where the function $f(x)$ is evaluated and $\Delta x_n = x_n - x_{n-1}$ is the step size [35–39]. In our case, the interval of integration and step size are taken as $[0, 100]$ and 1 respectively. During the numerical approximation, quantities like ω_{ce} , c , k_x , n , ω and η are treated as symbolic variables [44]. To approximate the integrals in equations (4) and (5), we use Wolfram Mathematica 10.

4. Discussions and graphical representations

To observe the characteristics of Ordinary waves in different electron plasma environments (relativistic, weakly relativistic and non-relativistic), we need to choose the values of η accordingly.

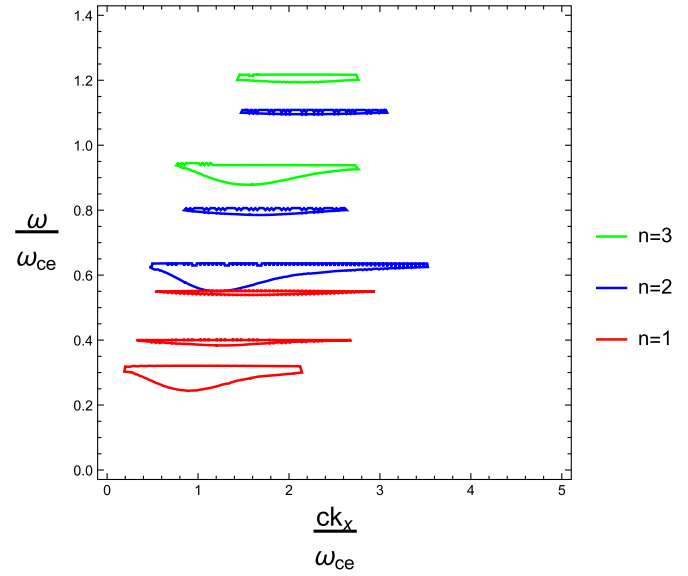


Figure 1. Dispersion curves showing the cyclotron harmonics for $\eta = 0.5$ and $\left(\frac{\omega_{pe}}{\omega_{ce}}\right)^2 = 25$ for Ordinary waves in relativistic plasma.

4.1. Cyclotron resonance

We will analyze the harmonic structure of the O-mode by plotting equation (3). If we reduce the propagation regime by keeping small values of the normalized frequency $\left(\frac{\omega}{\omega_{ce}}\right)$, we will get the cyclotron harmonic resonance structure for different values of η , which is explained below.

4.1.1. Cyclotron harmonic resonance structure in relativistic electron plasma.

When the thermal energy of the particles is greater or equal to the rest mass energy ($k_B T_e \geq mc^2$), cyclotron harmonic resonance structure of the Ordinary waves is strongly affected by the relativistic mass. In figure 1, a plot of the ordinary waves is presented for $\eta = 0.5$ and $\frac{\omega_{pe}^2}{\omega_{ce}^2} = 25$. Due to relativistic effects, the mass of particles increases depending upon the velocity. As a result, particles will gyrate at different cyclotron resonance frequencies even for the same harmonic number n . This effect can easily be observed in the dispersion curves. The first and second harmonic number n has three wave modes and the third contains two wave modes. The resonance curves in figure 2, are obtained for $\eta = 1$ and $\frac{\omega_{pe}^2}{\omega_{ce}^2} = 25$. When we increase the value of η from 0.5 to 1, the same number of wave modes exist for each harmonic number n , but now the wave modes are shifted to a higher value of frequency and also propagate for large k_x . By comparing figures 1 and 2, we can analyze the modification in the wave modes due to these relativistic effects.

4.1.2. Cyclotron harmonic resonance structure in weakly relativistic electron plasma.

In the weakly relativistic electron plasma, the thermal energy of the particles is less than the rest mass energy i.e. ($k_B T_e < mc^2$). In figure 3, the resonance curves are presented for $\eta = 6$ (weakly relativistic regime) and $\frac{\omega_{pe}^2}{\omega_{ce}^2} = 25$. Here we observe that the number of

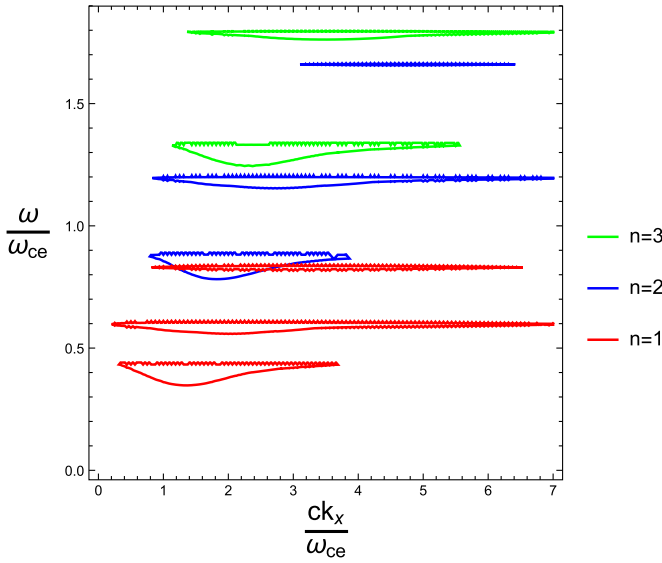


Figure 2. Dispersion curves showing the cyclotron harmonics for $\eta = 1$ and $(\frac{\omega_{pe}}{\omega_{ce}})^2 = 25$ for Ordinary waves in relativistic plasma.

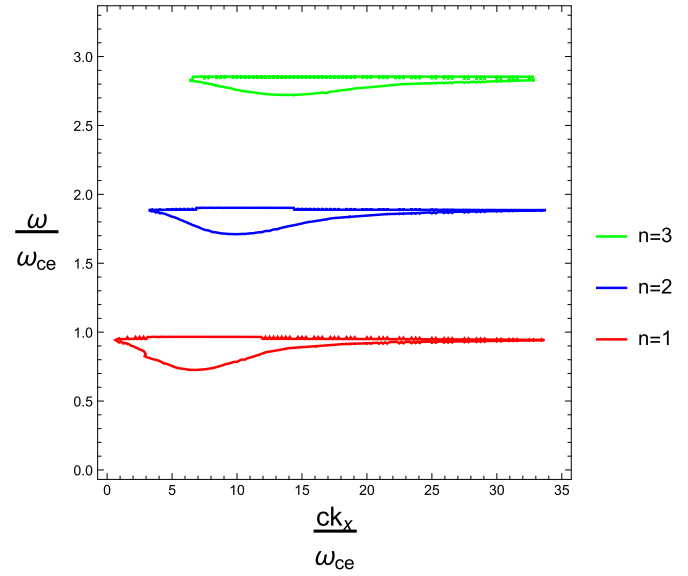


Figure 4. Dispersion curves showing the cyclotron harmonics for $\eta = 50$ and $(\frac{\omega_{pe}}{\omega_{ce}})^2 = 25$ for Ordinary waves in non-relativistic plasma.

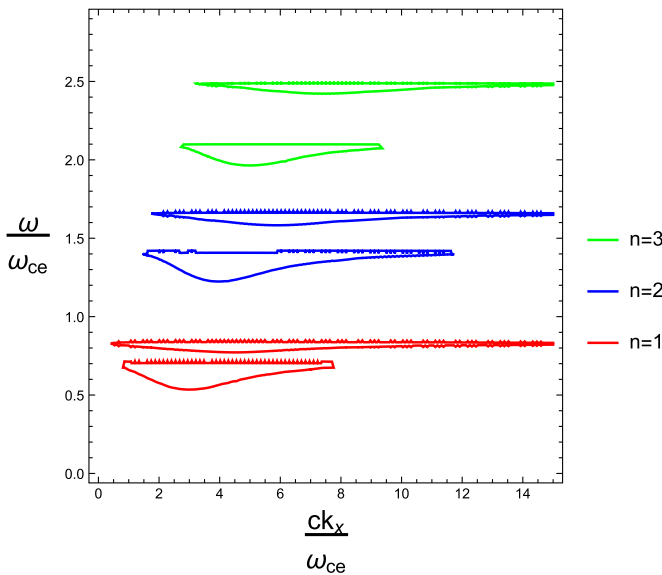


Figure 3. Dispersion curves showing the cyclotron harmonics for $\eta = 6$ and $(\frac{\omega_{pe}}{\omega_{ce}})^2 = 25$ for Ordinary waves in weakly relativistic plasma.

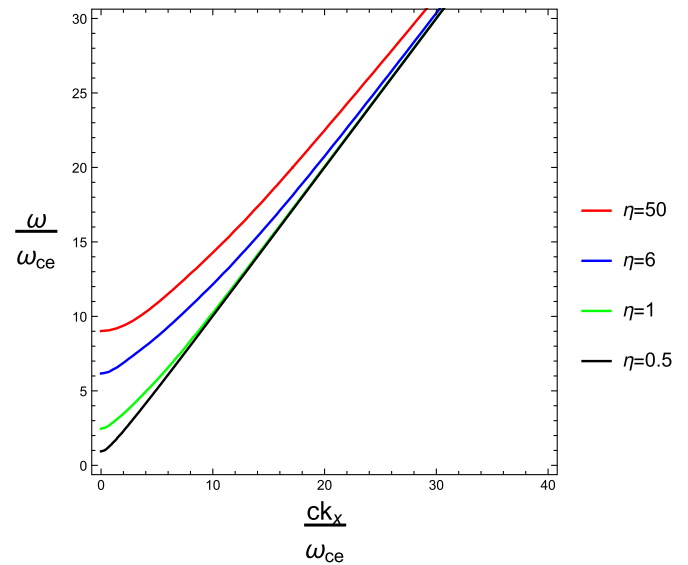


Figure 5. Dispersion curves showing propagation of ordinary waves for different values η and $(\frac{\omega_{pe}}{\omega_{ce}})^2 = 25$.

wave modes, corresponding to the harmonic number $n = 1$ and $n = 2$ decreases as expected. In weakly relativistic electron plasma, cyclotron resonance curves also shift to lower values but less as compared to the relativistic case.

4.1.3. Cyclotron harmonic resonance structure in non-relativistic electron plasma. In non-relativistic electron plasma, the thermal energy of the particles is very small as compared to the rest mass energy ($k_B T_e \ll mc^2$), so the relativistic effects do not play any role in the characteristic curves. In figure 4, a plot of the O-mode is presented for

$\eta = 50$ and $(\frac{\omega_{pe}}{\omega_{ce}})^2 = 25$. In the non-relativistic limit, we get only one wave mode for each harmonic number n .

4.2. Propagation

When we focus our attention on the large values of the normalized frequency ($\frac{\omega}{\omega_{ce}}$), we observe that the harmonic structure vanishes and we obtain a single curve for the O-mode. In the same way as before, we take different values of η to incorporate the relativistic effects and fix the value of $(\frac{\omega_{pe}}{\omega_{ce}})^2$ in figure 5. We can easily observe that when the value of η decreases, the plasma becomes more transparent for the O-mode.

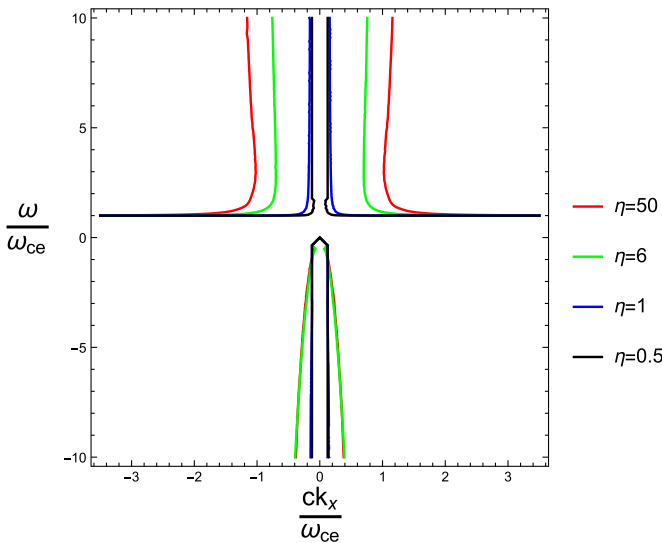


Figure 6. Dispersion curves showing the cutoffs of the ordinary waves for different values of η by taking $\frac{\omega_{pe}^2}{\omega_{ce}^2} = 25$.

4.3. Cutoffs

To analyze the relativistic effects on the cutoff points of the O-mode, we plot $(\frac{\omega^2}{c^2 k_x^2})$ vs $(\frac{\omega}{\omega_{pe}})$ in figure 6 for different values of η and by taking $\frac{\omega_{pe}^2}{\omega_{ce}^2} = 25$. Here we observe that the cutoff point is shifted to a higher value by increasing the value of η .

5. Conclusions

In this article, we analyze the ordinary waves in different plasma environments. Due to the momentum dependence of the cyclotron frequency in the relativistic and weakly relativistic electron plasma, we conclude that the cyclotron resonance wave modes are shifted to lower values of frequency and we obtain more than one wave mode corresponding to each harmonic number n , both in the relativistic and weakly relativistic case. The number of wave modes decreases when we go from the relativistic regime to the weakly relativistic regime. Eventually, we observe only one wave mode for each harmonic number n in the non-relativistic regime. The reason behind getting more than one wave mode is that the particles associated with each harmonic number n can have different relativistic velocities, so they oscillate at different cyclotron frequencies even for the same harmonic number n . In the non-relativistic limit, as there is no change in the mass of the particle or in other words the cyclotron frequency remains same for all particles, a single wave mode exists for each harmonic number n as expected. When we plot the dispersion curves for large values of $(\frac{\omega}{\omega_{ce}})$ vs $(\frac{ck_x}{\omega_{ce}})$ we observe that the plasma become more transparent for the O-mode at a high temperature.

ORCID iDs

Waseem Khan  <https://orcid.org/0000-0003-1069-3341>

M Ali  <https://orcid.org/0000-0003-1023-8648>

Yousaf Habib  <https://orcid.org/0000-0003-1709-1159>

References

- [1] Khan S 2012 *Phys. Plasmas* **19** 014506
- [2] Khan W, Ali M, Iqbal Z, Abbas G and Ehsan Z 2018 *Phys. Plasmas* **25** 102103
- [3] Chen F F 1984 *Introduction to Plasma Physics and Controlled Fusion* (Berlin: Springer)
- [4] Lightman A P 1982 *Astrophys. J.* **253** 842
- [5] Fidone I, Granata G and Meyer R L 1982 *Phys. Fluids* **25** 2249
- [6] Harvey R W, Nevins W M, Smith G R, Lloyd B, O'Brien M R and Warrick C D 1997 *Nucl. Fusion* **37** 69
- [7] Darbos C et al 2016 *J. Infrared Millim. Terahertz Waves* **37** 4
- [8] Farina D, Henderson M, Figini L and Saibene G 2014 *Phys. Plasmas* **21** 061504
- [9] Figini L, Decker J, Farina D, Marushchenko N B, Peysson Y, Poli E and Westerhof E 2012 *EPJ Web Conf.* vol 32 p 01011
- [10] Henderson M et al 2009 *34th Int. Conf. on Infrared, Millimeter and Terahertz Waves* IEEE 1
- [11] Henderson M et al 2015 *Phys. plasmas* **22** 021808
- [12] Omori T et al 2015 *Fusion Eng. Des.* **96** 547
- [13] Youchison D L, Melin A M, Lumsdaine A, Schaich C R and Hanson G R 2017 *Fusion Sci. Technol.* **72** 324
- [14] Seol J, Park B H, Kim S S, Kim J Y and Na Y S 2010 *Nucl. Fusion* **50** 105008
- [15] Shukla B K, Patel J, Mistry H, Patel H, Purohit D, Parmar K G, Babu R, Ghosh J, Tanna R, Jadeja K and Patel K 2019 Commissioning of electron cyclotron resonance heating (ECRH) system on tokamak Aditya-U *Fusion Eng. Des.*
- [16] Krall N A and Trivelpiece A W 1973 *Principles of Plasma Physics* (New York: McGraw-Hill)
- [17] Kallenrode M B 2013 *An Introduction to Plasmas and Particles in the Heliosphere and Magnetospheres* (Berlin, Germany: Springer Science and Business Media)
- [18] Nambu M 1974 *Phys. Fluids* **17** 1885
- [19] (<https://www.iter.org/mach/Heating>)
- [20] (<https://en.wikipedia.org/wiki/Tokamak#Radio-frequency-heating>).
- [21] Ali M, Khan W and Ehsan Z 2019 *Phys. Plasmas* **26** 102101
- [22] Hansen F, Lynov J P and Michelsen P 1985 *Plasma Phys. Controlled Fusion* **27** 1077
- [23] Fidone I, Granata G, Ramponi G and Meyer R L 1978 *Phys. Fluids* **21** 645
- [24] Zaheer S and Murtaza G 2008 *Phys. Scr.* **77** 035503
- [25] López R A, Moya P S, Muñoz V, Viñas A F and Valdivia J A 2014 *Phys. Plasmas* **21** 092107
- [26] Iqbal Z, Hussain A, Murtaza G and Tsintsadze N L 2014 *Phys. Plasmas* **21** 032128
- [27] Kalsoom A, Muddasir A and Hussain A 2017 *Plasma Sci. Technol* **18** 035001
- [28] Abbas G, Bashir M F and Murtaza G 2012 *Phys. Plasmas* **19** 072121
- [29] Ali M, Zaheer S and Murtaza G 2010 *Prog. Theor. Phys.* **124** 1083
- [30] Nikolic L and Pesic S 1998 *Plasma Phys. Control* **40** 1373
- [31] Weiss I 1985 *J. Comput. Phys.* **61** 403
- [32] Bell W W 2004 *Special Functions for Scientists and Engineers* (North Chelmsford, Chelmsford, Massachusetts, United States: Courier Corporation)

- [33] Georgiou A 1996 *Plasma Phys. Controlled Fusion* **38** 347
- [34] Buti B 1963 *Phys. Fluids* **6** 89
- [35] Burden R L and Faires J D 1997 *Numerical Analysis* (Pacific Grove, CA: Brooks/Cole Publishing) vol 7
- [36] Chapra S C and Canale R P 2010 *Numerical Methods for Engineers* (New York: McGraw-Hill Higher Education)
- [37] Evans G 1993 *Practical Numerical Integration* (New York: Wiley)
- [38] Yang X S 2014 *Introduction to Computational Mathematics* (Singapore: World Scientific Publishing Company)
- [39] Zimmermann P, Casamayou A, Cohen N, Connan G, Dumont T, Fousse L, Maltey F, Meulien M, Mezzarobba M, Pernet C and Bray E 2018 *Computational Mathematics With Sagemath* (Philadelphia, PA: SIAM)
- [40] Castejón F and Pavlov S S 2006 *Phys. plasmas* **13** 072105
- [41] Swanson D G 2012 *Plasma Waves* (Amsterdam: Elsevier)
- [42] Stix T H 1992 *Waves in Plasmas* (London, Heidelberg: Springer Science and Business Media)
- [43] Weiss I 1985 *J. Comput. Phys.* **61** 403–16
- [44] Waseem K *et al* 2020 *Plasma Res. Express* **2** 015004